Replication-Uncoupled Histone Deposition during Adenovirus DNA Replication

doi: 10.1128/JVI.00380-12

Replication-uncoupled histone deposition during adenovirus DNA replication

Tetsuro Komatsu and Kyosuke Nagata*

Department of Infection Biology, Faculty of Medicine and Graduate School of Comprehensive Human Sciences, University of Tsukuba, Tsukuba 305-8575, Japan

*Corresponding author. Department of Infection Biology, Faculty of Medicine and Graduate School of Comprehensive Human Sciences, University of Tsukuba, 1-1-1 Tennodai, Tsukuba 305-8575, Japan. Phone and fax: (81) 298-53-3233. E-mail: knagata@md.tsukuba.ac.jp.

Running title: DBP and histone H3.3 in adenovirus DNA replication

ABSTRACT: 203 words

TEXT: 5255 words

ABSTRACT

In infected cells, the chromatin structure of the adenovirus genome DNA plays critical roles in its genome functions. Previously, we have reported that in early phases of infection, incoming viral DNA is associated with both viral core protein VII and cellular histones. Here we show that in late phases of infection, newly synthesized viral DNA is also associated with histones. We also found that knockdown of CAF-1, a histone chaperone that functions in replication-coupled deposition of histones, does not affect the level of histone H3 bound on viral chromatin, although CAF-1 is accumulated at viral DNA replication foci together with PCNA. Chromatin immunoprecipitation assays using epitope-tagged histone H3 demonstrated that histone variant H3.3, which is deposited onto the cellular genome in a replication-independent manner, is selectively associated with both incoming and newly synthesized viral DNAs. Microscopic analyses indicated that histones but not USF1, a transcription factor that regulates viral late gene expression, are excluded from viral DNA replication foci and this is achieved by oligomerization of DBP. Taken together, these results suggest that the histone deposition onto newly synthesized viral DNA is most likely uncoupled with viral DNA replication, and a possible role of DBP oligomerization in this replication-uncoupled histone deposition is discussed.

INTRODUCTION

In the cell nucleus, the genomic DNA is not naked, but forms chromatin structure with chromatin proteins. The fundamental unit of the chromatin structure is a nucleosome, which consists of histone octamer (two copies each of histone H2A, H2B, H3, and H4) and DNA wrapping around the octamer. Deposition of histones and/or remodeling of nucleosome arrays are critical processes for the expression of genome functions (2), since nucleosome packaging could be barrier for *trans*-acting factors to access their cognate sites on DNA. Thus, the nucleosome structure must be strictly and dynamically regulated in connection with several events on chromatin, such as transcription, DNA replication, and DNA repair.

Currently, it is known that histone deposition is carried out mainly by two fashions, DNA replication-dependent and independent ones, and a role of histone variants in these deposition pathways has been elucidated (14). In mammalian somatic cells, there are three major histone H3 variants, H3.1, H3.2, and H3.3, and they have only slight differences in amino acid (aa) sequences (16). The canonical histone H3, histone H3.1 and highly related variant H3.2 (which differs only 1 aa from H3.1) are expressed exclusively during S phase, while the expression of the variant H3.3 that differs 4 and 5 aa from H3.2 and H3.1, respectively, is observed throughout cell cycle. Thus, this variant is called “replication-independent” one (11). Tagami *et al.* demonstrated that the canonical histone H3 (H3.1) interacts with histone chaperone CAF-1 complex and is deposited onto DNA in a replication-dependent manner, while HIRA specifically binds to and deposits histone variant H3.3 onto DNA independently

of DNA synthesis (43). CAF-1 is composed of three subunits, p150, p60, and p48, and associated with the cellular DNA replication machinery through the interaction with PCNA, a sliding clamp for DNA polymerases, allowing DNA replication-coupled deposition of histones (40, 41, 50). On the other hand, HIRA was identified as a DNA synthesis-independent histone chaperone by *cell-free* systems using *Xenopus* egg extracts (32), and histone variant H3.3 is shown to mark transcriptional active genomic regions (1). Furthermore, additional H3.3-specific chaperones are recently identified. Daxx is one of components of PML nuclear bodies and reported to deposit histone H3.3 onto the specific genomic regions such as telomeres and pericentric heterochromatin, together with an ATP-dependent chromatin remodeler, ATRX (10, 21). It is also reported that in *Drosophila* cells, DEK is a coactivator of a nuclear receptor and functions as an H3.3-specific chaperone (37). Thus, the mechanistic evidences for histone deposition are accumulating, in the case of cellular chromatin.

The regulatory events for chromatin structure are not limited to the cellular genome, as some viruses also have chromatin and/or chromatin-like structures with their own genomes. The adenovirus (Ad) genome is a liner double-stranded DNA (dsDNA) of ~36000 bp in length. In the virion, the Ad genome forms chromatin-like structure with viral basic core proteins, as it is revealed by electron microscopic analyses that viral core protein-DNA complexes purified from the virion show "beads-on-a-string" structure (49). Among core proteins, protein VII is a major DNA binding protein that can introduce superhelical turns into DNA as do cellular histones (4), and remains associated with viral DNA after the entry of the nucleus (7, 17).

When viral DNA-core protein complexes purified from the virion are used as a template for *cell-free* DNA replication/transcription systems, the reactions occur at a much lower level, compared with the case of naked DNA, indicating that viral chromatin-like structure must be remodeled to execute its genome functions (22, 23). Previously, we have identified host cell-derived remodeling factors for Ad chromatin with biochemical analyses (19, 22, 24, 26) and demonstrated that TAF-I, one of these host factors, plays an important role in the regulation of viral early gene expression in infected cells through the interaction with protein VII (15, 17, 18, 20, 27). Thus, it is indicated that remodeling of Ad chromatin is a crucial process for its genome functions (13), as is the case for the cellular genome. In addition, recently we have reported using chromatin immunoprecipitation (ChIP) assays that in early phases of infection, cellular histones are incorporated into viral DNA-protein VII complexes and histone modification occurs depending upon transcription states on viral chromatin, suggesting that cellular histones could be functional components of viral chromatin in infected cells (20).

As described above, although viral chromatin structure and its regulation in early phases of infection are being clarified, it is quite unclear how viral chromatin structure is regulated in late phases of infection. In particular, since the expression of viral late genes is largely dependent on its own DNA replication (45), the regulation of the chromatin structure during viral DNA replication could be a key step. Therefore, in this study we sought to elucidate the regulatory mechanism how the chromatin structure is formed on newly synthesized viral DNA through viral DNA replication, in particular with respect to the histone deposition. We found that after the onset of viral

DNA replication, cellular histones are also incorporated into viral chromatin. We also found that although CAF-1 is accumulated at the site of viral DNA replication, this factor seems not to be involved in the histone deposition during viral DNA replication, since knockdown of CAF-1 did not affect the binding level of histone H3 on viral chromatin and histone variant H3.3, which is deposited onto DNA in a DNA synthesis-independent manner, is specifically deposited onto viral DNA even after the onset of viral DNA replication. Microscopic analyses suggest that histones but not USF1, a transcription factor which is shown to bind to and regulate transcription from viral major late promoter (MLP) (46), are excluded form the site of viral DNA replication, possibly by oligomerization of Ad single-stranded DNA (ssDNA) binding protein (DBP), one of viral DNA replication factors. Based on these results, we would propose a model that unlike cellular chromatin, the histone deposition onto the newly synthesized viral DNA is not coupled with viral DNA replication. A feasible role of this uncoupled deposition mechanism mediated by DBP oligomerization on Ad genome functions is discussed.

MATERIALS AND METHODS

Cells and viruses.

Maintenance of HeLa cells, and purification and infection of human adenovirus type 5 (HAdV5) were carried out essentially as described previously (18, 20). Hydroxyurea (HU) was added at the final concentration of 2 mM right after infection when DNA replication was to be blocked. HeLa cells stably expressing EGFP-tagged histone H3.2 and H3.3 [a kind gift from Dr. M. Okuwaki (University of Tsukuba)] were also maintained as described above. Transfection of expression plasmids was performed using GeneJuice (Novagen) according to the manufacturer's protocol.

Antibodies.

Antibodies used in this study are as follows: rabbit anti-histone H3 (catalog no. ab1791; abcam), rabbit anti-histone H4 (catalog no. 04-858; Millipore), rabbit anti-histone H2A (catalog no. ab18255; abcam), mouse anti-HIRA (catalog no. 04-1488; Millipore), mouse anti-FLAG M2 (catalog no. F3165; Sigma), rat anti-HA (3F10; Roche), and mouse anti-β-actin (Sigma) antibodies. Rabbit anti-histone H2A-H2B, mouse anti-CAF-1 p150, and mouse anti-DBP antibodies were kindly provided by Dr. M. Okuwaki (University of Tsukuba), Dr. A. Verreault (University of Montreal), and Dr. W. C. Russel, respectively. Rat anti-protein VII antibody was described elsewhere (17).

Vector construction.

To construct the expression vectors for USF1, full-length DBP, and its deletion mutant (DBPΔC, which lacks the C-terminal 17 aa), cDNA fragments of USF1, DBP, and DBPΔC were amplified by PCR, digested with BamHI and EcoRI, and cloned in-frame into pCHA vector containing a hemagglutinin (HA) epitope tag and the puromycin-resistance gene [pCHA-puro vector, kindly provided from K. Kajitani (University of Tsukuba)]. The resulting vectors are designated pCHA-puro-USF1, pCHA-puro-DBP, and pCHA-puro-DBPΔC, respectively. Similarly, for the expression vector of PCNA, amplified cDNA fragment was digested with BamHI and cloned into pCHA-puro vector digested with BamHI and EcoRV (pCHA-puro-PCNA). The primers used here were as follows: 5’-GTTTAGGATCCCATATGAAGGGGCAGCAG-3’ and 5’-GGGCCGAATTCTTAGTTGCTGTCATTCTTG-3’ for USF1 cDNA, 5’-AAAGGATCCATGGCCAGTCGGG-3' and 5’-GCGGAATTCTTAAAAATCAAAGGGGTTCTG-3' for DBP cDNA, 5’-AAAGGATCCATGGCCAGTCGGG-3' and 5’-CCCGAATTCTTAGTTGCGATACTGG-3' for DBPΔC cDNA, and 5’-AAAGGATCCATGTTCGAGGCGC-3' and 5’-ATCGTCGACCTAAGATCCTTCTTC-3' for PCNA cDNA.

For preparation of cells stably expressing HA-PCNA, HeLa cells were transfected with pCHA-puro-PCNA and cultured in the presence of 2 μg/mL puromycin for 2 weeks.

For construction of the expression vector of histone H3.1, cDNA fragment of histone H3.1 was amplified by PCR, digested with NcoI, and cloned into pBS-FLAG vector (pBS-H3.1-FLAG). Then, the DNA fragment containing cDNA of H3.1 and the C-terminal FLAG tag was obtained from pBS-H3.1-FLAG by digestion with BamHI and EcoRI, and cloned into pcDNA3 vector (pcDNA3-H3.1-FLAG). The primers used here were as follows: 5'-AAAACCATGGCGCGTACTAAGCAG-3' and 5'-TTATTCCATGGCCGCCCTCTCCCCA-3'.

The expression vectors for FLAG-tagged histone H3.2 and H3.3 (pcDNA3-H3.2-FLAG and pcDNA3-H3.3-FLAG) and HA-tagged DEK (pCHA-DEK) were generously provided by Dr. M. Okuwaki and Dr. S. Saito, respectively (University of Tsukuba).

Indirect immunofluorescence assays.

Indirect immunofluorescence (IF) assays were carried out essentially as previously described (18). Localization of the protein was visualized with the secondary antibodies (anti-mouse IgG conjugated with AlexaFluor 488, anti-mouse IgG conjugated with AlexaFluor 568, and anti-rabbit IgG conjugated with AlexaFluor 568; Invitrogen). DNA was visualized by staining with TO-PRO-3 iodide (Invitrogen). Labeled cells were observed with confocal laser scanning microscopy (LSM5 Exciter; Carl Zeiss) using argon laser (488 nm) and He/Ne laser (546 and 633 mm) lines.

ChIP, RT-PCR, siRNA-mediated knockdown, and western blot assays.

These experiments were carried out essentially as described previously (20). siRNA targeted for CAF-1 p150 was commercially purchased (Stealth siRNA; Invitrogen). Primers for *CAF-1 p150* mRNA are as follows: 5'-GGAGCAGGACAGTTGGAGTG-3' and 5'-GACGAATGGCTGAGTACAGA-3'. Other primers for ChIP and RT-PCR assays were described elsewhere (20). In all the experiments by quantitative PCR (qPCR), mean values with SD were obtained from three independent experiments.

RESULTS

Cellular histones are bound with viral chromatin both in early and late phases of infection.

Previously, we reported that in early phases of infection (before the onset of viral DNA replication), viral chromatin is composed of both viral core protein VII and cellular histones and this "chimeric" chromatin functions as template for transcription (20). To examine whether histones are also bound with viral chromatin after the onset of viral DNA replication, we performed ChIP assays using antibodies against histones and protein VII (Fig. 1). The viral DNA replication starts around 8 hpi (hours post infection) in our condition (17, 20). In order to reveal the viral chromatin state during/right after viral DNA replication, HeLa cells infected at an MOI (multiplicity of infection) of 100 were harvested at 6 and 12 hpi for ChIP assays. We chose five regions for ChIP assays, four viral genome regions (E1A pro, MLP, Hexon, E4 pro, Fig. 1A) and one cellular genomic region (ribosomal RNA gene, rDNA) as a control (20). In this condition, the amount of viral DNA was increased by ~20 fold through viral DNA replication (Fig. 1B). At 6 hpi, all core histones are bound with viral chromatin, but at the low binding level compared with cellular chromatin (Fig. 1C, histone H3, H4, and H2A-H2B). This was in good agreement with our previous observation (20). At 12 hpi, core histones were also found to be associated with viral chromatin. The binding level of histones on viral chromatin at 12 hpi was more than those at 6 hpi, but slightly less than those on cellular chromatin. This is consistent with the previous report of electron microscopic analyses showing that viral genome DNA purified from

infected cells at late phases of infection has the nucleosome-like particles, which are less dense compared with cellular nucleosome arrays (3). In contrast, the binding level of protein VII was drastically decreased after the onset of viral DNA replication (Fig. 1C, protein VII), suggesting that newly synthesized viral DNA is mainly associated with cellular histones. We do not exclude the possibility that protein VII remains associated with small population of viral chromatin because the binding level of protein VII on viral chromatin was still higher than that on cellular chromatin even at 12 hpi. The ratio among core histones bound on viral chromatin was almost the same as that on cellular chromatin both at 6 (data not shown, 20) and 12 hpi (Fig. 1D), indicating that viral chromatin contains the canonical nucleosome structure.

CAF-1 and PCNA are not involved in the histone deposition onto newly synthesized viral DNA.

It is known that during DNA replication of the cellular genome and some DNA virus genomes, histones are deposited by CAF-1, a replication-dependent histone chaperone (41, 43). CAF-1 is associated with the DNA replication machinery through the interaction with PCNA, thereby enabling replication-coupled deposition of histone H3-H4 complexes (40). Thus, it is worthwhile to examine whether CAF-1 and PCNA are also involved in the histone deposition onto newly synthesized Ad DNA, although there is no definitive evidence that those two are involved in the Ad DNA replication. To test this, we first performed IF assays using cells stably expressing HA-tagged PCNA (HA-PCNA) to examine the relationship among viral DNA replication, PCNA,

236 and CAF-1 (Fig. 2A). Using antibody against DBP, Ad ssDNA binding protein
237 involved in viral DNA replication, the place for viral DNA replication designated “viral
238 DNA replication foci” (hereafter referred to as “VDRF”) can be visualized (31). HeLa
239 cells or cells stably HA-PCNA were infected at an MOI of 50, and at 18 hpi subjected to
240 IF assays using anti-DBP and anti-HA antibodies. In mock-infected cells, HA-PCNA
241 was localized throughout the nucleus and shows the punctate localization in some cell
242 population, as reported previously (29). At 18 hpi, VDRF was observed as a
243 donut-like signal using anti-DBP antibody, and we found that HA-PCNA showing
244 punctate localization was accumulated inside VDRF. We also observed the similar
245 localization pattern of CAF-1 inside VDRF (see below in Fig. 4A). These results
246 suggest that PCNA and CAF-1 are recruited together into the site of viral DNA
247 replication.

248 Next, to investigate a role of CAF-1 in the histone deposition onto viral DNA,
249 siRNA-mediated knockdown of CAF-1 p150, a largest subunit of CAF-1 complex, was
250 carried out (Fig. 2B, C, and D). HeLa cells were treated with control siRNA (siCont)
251 or siRNA for CAF-1 p150 (siCAF-1), infected with HAdV5 at an MOI of 100, and
252 harvested at 6 and 12 hpi. First, we examined the knockdown efficiency of CAF-1
253 p150 by RT-qPCR assays (Fig. 2B). The mRNA level of CAF-1 p150 in
254 siRNA-treated cells was about 20% of those in control cells, although at 12 hpi the level
255 was slightly increased possibly due to S-phase like environment induced by Ad
256 infection (30). In contrast, the mRNA level of GAPDH was almost unaffected by
257 siRNA treatment and Ad infection. In this condition, the binding level of histone H3

on viral chromatin was examined by ChIP assays (Fig. 2C). The binding level of H3 on viral chromatin was not decreased by CAF-1 knockdown, and rather slightly increased (but not statistically significant) at 12 hpi (Fig. 2C, E1A pro and MLP). It is noted that the binding level of H3 on cellular chromatin was also unaffected by CAF-1 knockdown (Fig. 2C, rDNA, see Discussion). In addition, we could not observe any effect of CAF-1 knockdown on viral DNA replication levels (Fig. 2D). Taken together, these results suggest that it is not likely that CAF-1 is involved in the histone deposition onto viral chromatin during viral DNA replication, although CAF-1 is accumulated at VDRF together with PCNA.

Replication-independent histone H3.3 is selectively incorporated into viral chromatin.

It is known that among histone H3 variants, histone H3.1 and H3.2 are deposited onto DNA by CAF-1 during DNA replication, while H3.3 is deposited independently of DNA replication (11, 14). If CAF-1 is not involved in the histone depostion during viral DNA replication, histone H3.3 rather than H3.1 and H3.2 could be incorporated into newly synthesized viral DNA. Therefore, to examine this possibility, we performed ChIP assays using FLAG-tagged histone H3.2 and H3.3 (Fig. 3). HeLa cells were transfected with expression vectors for H3.2 and H3.3 and at 24 hpt (hours post transfection) infected at an MOI of 100. We first studied using cells at early phases of infection (before the onset of viral DNA replication) (Fig. 3A). Infected cells were harvested at 2 and 6 hpi, and at 10 hpi in presence of HU to block

viral DNA replication (20), and subjected to ChIP assays with anti-FLAG antibody. As shown in Figure 3A, the exclusive binding of H3.3 on viral chromatin was observed at all the regions we tested, with a gradual increment as infection proceeded. This is consistent with the recent report on helper-dependent Ad vector (HdAd) indicating that histone H3.3 are specifically deposited onto HdAd DNA by HIRA, an H3.3-specific histone chaperone (34). Since HdAd alone does not undergo its DNA replication, the chromatin state of HdAd may reflect that of wildtype Ad in early phases of infection (13, 34).

Next we performed ChIP assays at 12 hpi to examine which H3 variant is deposited onto newly synthesized viral DNA (Fig. 3B). We found that histone H3.3 but not H3.2 was associated with viral chromatin at this time point, as observed in early phases of infection. The expression levels of both H3 variants were comparable (Fig. 3C), and both variants were associated with cellular chromatin with a similar binding level (Fig. 3A and B, rDNA). These strongly suggest that this result was not due to some technical issues. Further, we obtained the same results by using FLAG-tagged histone H3.1 instead of H3.2 (Fig. 3D and E). Thus, these results suggest that replication-independent histone variant H3.3 is selectively deposited onto not only incoming but also newly synthesized viral DNA in infected cells.

Histones but not transcription factor USF1 are excluded from the site of viral DNA replication.

To further investigate the histone fluctuation during viral DNA replication, we

302 performed IF analyses using HeLa cells stably expressing EGFP-tagged histone H3.3
303 (Fig. 4A). Cells were infected at an MOI of 50, and at 18 hpi subjected to IF assays
304 using anti-DBP antibody (Fig. 4A, upper panels). VDRF was observed at 18 hpi as
305 described above, and H3.3-EGFP was found to be excluded from VDRF. Similar
306 results were obtained by using cells stably expressing EGFP-tagged histone H3.2 (Fig.
307 4B). This was due to neither exogenous expression nor EGFP tag of H3 variants as we
308 observed the similar exclusion of the endogenous histone using anti-histone H2A
309 antibody (Fig. 4C). This localization pattern was specific for late phases of infection
310 since the localization of EGFP-tagged H3 variants was not changed in early phases of
311 infection (Fig. 4D). We also performed IF analyses using anti-CAF-1 p150 antibody
312 and observed that CAF-1 was accumulated at “histone-less” region, that is, VDRF (Fig.
313 4A, lower panels), as was observed with HA-PCNA (Fig. 2A). In summary, these
314 results indicated that histones are localized reciprocally to VDRF (and CAF-1/PCNA)
315 in late phases of infection.

316 To gain more insights into the accessibility of other nuclear proteins to VDRF,
317 we again performed IF analyses (Fig. 5). First, IF analyses were carried out using
318 antibody against HIRA, an H3.3-specific histone chaperone, and it was observed that
319 the localization of HIRA was not drastically changed in both early and late phases of
320 infection (Fig. 5A). We also performed IF analyses using cells transiently transfected
321 with expression vectors for HA-tagged DEK and USF1 (Fig. 5B and C). DEK is a
322 cellular chromatin protein with potential histone chaperone activity (37), and USF1 is
323 an E-box-binding transcription factor and reported to bind to and regulate transcription

from the MLP region (46). HeLa cells were transfected with expression vectors and at 24 hpt subjected to western blot analyses (Fig. 5B) or infected at an MOI of 50. At 18 hpi, localization of DBP, HA-DEK, and HA-USF1 was visualized by IF analyses using anti-DBP and anti-HA antibodies (Fig. 5C). In mock-infected cells, both HA-tagged proteins showed nuclear localization, and in the case of HA-DEK, a strong signal was observed at the nuclear periphery. At 18 hpi, HA-DEK appeared to be excluded from VDRF (Fig. 5C, HA-DEK). However, in contrast to HA-DEK, we observed that HA-USF1 could be localized inside VDRF (Fig. 5C, HA-USF1). Taken together, our IF analyses suggest that VDRF may allow selective access of cellular nuclear proteins, and at least one of transcription factors, USF1, is able to access the inside of VDRF.

Oligomerization of DBP is critical for the histone exclusion from VDRF.

To investigate the mechanism of the histone exclusion from VDRF, we hypothesized that DBP may play a role, since an abundant amount of DBP is associated with Ad DNA in VDRF. The crystal structure of DBP revealed that this protein has a 17 aa extension at its C-terminus (see Fig. 6A), and this C-terminal “arm” hooks onto the next DBP molucule, resulting in oligomerization of DBP (47). It was also reported that oligomerization of DBP mediated by the C-terminal “arm” enables ATP-independent unwinding of dsDNA, and thus full-length DBP, but not the deletion mutant that lacks the C-terminal “arm” (DBPΔC), could support viral DNA replication *in vitro* (9). Therefore, to examine a role of DBP and its oligomerization on the histone localization, HeLa cells expressing histone H3.3-EGFP were transfected with

346 the expression vectors for HA-tagged full-length DBP or DBPΔC and at 36 hpt
347 subjected to western blotting and IF assays using anti-HA and anti-DBP antibodies (Fig.
348 6B and C). The expression levels of both DBP proteins were almost the same as
349 indicated by western blotting (Fig. 6B). In IF analyses, we observed that full-length
350 DBP forms the foci like VDRF in the absence of any viral proteins/DNA, and histone
351 H3.3-EGFP was excluded from these foci as observed in infected cells (Fig. 6C,
352 HA-DBP). In sharp contrast, DBPΔC was localized throughout the nucleus and did
353 not form such foci (Fig. 6C, HA-DBPΔC). Taken together, these results suggest that
354 the oligomerization of DBP has a critical role in the histone exclusion from VDRF.
355
356

DISCUSSION

In this study we showed that replication-independent histone variant H3.3 is deposited onto both incoming and newly synthesized Ad DNA (Fig. 3). These results, together with the results from knockdown experiments of CAF-1 (Fig. 2) and microscopic analyses (Figs. 4, 5, and 6), indicated that the histone deposition onto the replicated virus genome is most likely uncoupled with viral DNA replication. Based on these results, together with the previous our work (20), we hypothesize a model with respect to the fluctuation of viral chromatin structure during infection cycle (Fig. 7). In virions, viral DNA is tightly packed with viral core proteins (13). After the entry to the cell, cellular histones are incorporated into incoming viral DNA-protein VII complexes in the nucleus, and viral chromatin composed of both protein VII and histones functions as template for viral early gene expression (20). In this process, histone H3.3 is specifically deposited onto viral DNA, possibly by a histone chaperone HIRA (34). As infection proceeds and then viral DNA replication is initiated, oligomerization of DBP establishes the "histone-free" environment for viral DNA replication. Newly synthesized viral DNA is then associated with histone H3.3 in a replication-uncoupling fashion and might be acting as template for viral late gene expression outside VDRF (31). In later phases of infection (24~ hpi), both histones and newly synthesized core proteins VII and V are associated with viral DNA, which likely reflects the processes during the progeny virion assembly (35). Since histones are not included in virions, histones must be removed and replaced with newly synthesized core proteins for progeny virions. Although the packaging mechanism of

379 progeny viral DNA during virion assembly remains unclear, we have reported the
380 involvement of a nucleolar protein B23/nucleophosmin in the regulation of viral
381 chromatin structure during progeny virion assembly (35, 36).

382 The mechanistic details of the histone deposition after viral DNA replication
383 remain still unclear. First, what factor(s) is involved in the histone deposition at late
384 phases of infection? HIRA is a potential candidate for this process, likewise in early
385 phases of infection (34). However, we did not perform knockdown experiments for
386 HIRA, since even if we could observe some effect of HIRA knockdown on viral
387 chromatin in late phases of infection, we could hardly distinguish whether the
388 knockdown directly affects the chromatin structure of progeny viral DNA or the effect
389 is derived indirectly from earlier events on incoming viral chromatin. IF analyses
390 showed that the localization of HIRA was not drastically changed during infection cycle
391 (Fig. 5A). Recent reports indicated that Daxx, a component of PML bodies, is also an
392 H3.3-specific histone chaperone (10, 21). However, Daxx seems not to function the
393 H3.3 deposition onto viral DNA because during Ad infection, some components of PML
394 bodies including Daxx are re-localized by viral protein E4orf3, possibly for inactivation
395 of the components (6, 42). Indeed, it is shown that Daxx-mediated antiviral response
396 is antagonized by E4orf3 (48). It is also revealed that Daxx negatively functions and
397 undergoes E1B-55K- and proteasome-dependent degradation during Ad infection (39).
398 Furthermore, most recently Schreiner *et al.* reported that during/immediately after
399 nuclear import of incoming virus genome, protein VI, one of capsid proteins, binds to
400 and counteracts Daxx, at least partly by displacing it from PML bodies (38). These

401 reports strongly suggest that Daxx is inactivated entirely throughout infection cycle by
402 viral proteins. DEK is also recently reported as a chaperone for histone H3.3 in
403 *Drosophila* cells (37), but it is unknown whether human DEK also functions as a
404 variant-specific chaperone or not. Our IF analyses indicated that exogenously
405 expressed DEK is excluded from VDRF (Fig. 5B and C). Further studies are needed
406 to elucidate the functions of these factors in late phases of infection.

407 In this study, we could not observe a role of CAF-1 in the histone deposition
408 onto viral DNA, while the accumulation of CAF-1 at VDRF was observed (Figs. 2 and
409 4A). CAF-1 knockdown did not affect the binding levels of histone H3 on viral
410 chromatin (Fig. 2C). Although we could not exclude the possibility that the
411 knockdown efficiency of CAF-1 is not sufficient in the condition employed here, we
412 concluded that the function of CAF-1 is largely inhibited under our condition: We
413 observed that siCAF-1-treated cells exhibit aberrant cell shapes (data not show) and the
414 knockdown affects viral gene expression (see below). Second, histone H3.3 is
415 selectively incorporated into viral chromatin (Fig. 3), while CAF-1 generally functions
416 as a chaperone for H3.1 and H3.2 (43). Third, although CAF-1 is reported to be able
417 to be associated with H3.3 under some specific conditions (10, 21), we could not
418 observe any interaction between CAF-1 and H3.3 during Ad infection, at least, in our
419 experimental conditions (data not shown). In addition to their roles during DNA
420 replication, CAF-1 and PCNA are also reported to be involved in the DNA damage
421 response pathway (29). Carson *et al.* reported that the DNA damage response pathway
422 is only partially activated during Ad infection, and some related factors, such as ATRIP

423 and TopBP1, are accumulated at VDRF (5). Therefore, CAF-1 (and PCNA) might
424 localize at VDRF in the course of this limited DNA damage response. Recently, it was
425 reported that FACD2, one of factors involved in the DNA damage response, is
426 accumulated at VDRF, and loss of this protein results in less expression of viral late, but
427 not early, genes (8). Similarly, we observed that CAF-1 knockdown affects mRNA
428 levels of viral late genes without any effect on viral DNA replication (unpublished
429 observation). Thus, factors related to the DNA damage response such as FANCD2 and
430 CAF-1 might be required for viral late gene expression, although the underlying
431 mechanisms are unknown. In our condition, CAF-1 knockdown did not affect the
432 binding level of histone H3 on cellular chromatin (Fig. 2C, rDNA). This is consistent
433 with the report that loss of CAF-1 impairs replication-coupled deposition of histones but
434 the formation of nucleosome arrays on genomic DNA is still observed in the absence of
435 CAF-1 (44). In addition, a recent report demonstrated that a defect of histone H3.1
436 deposition by CAF-1 depletion could be rescued by HIRA-mediated H3.3 deposition
437 (33). Thus, in the case of cellular chromatin, alternative histone deposition pathway(s)
438 could rescue the loss of CAF-1 function.

439 It remains to be clarified what is the biological/virological significance of
440 histone deposition uncoupled with viral DNA replication. On cellular chromatin, a
441 replication-dependent histone chaperone CAF-1 is associated with the DNA replication
442 machinery and deposits histone H3.1-H4 (and H3.2-H4) complexes during DNA
443 replication (14, 40, 43). This DNA replication-coupled system of the histone
444 deposition is thought to be also utilized by some DNA viruses. For instance, DNA

445 replication of SV40 is largely depending on the cellular replication machinery, and
446 indeed CAF-1 was originally identified using *cell-free* DNA replication systems of
447 SV40 (41). In cytomegalovirus infection, it is reported that cellular histones, CAF-1,
448 and PCNA are accumulated at viral replication compartments (25). In the case of
449 herpes simplex virus type 1, it is shown that histone H3.3 is first deposited onto
450 incoming viral DNA by HIRA, and then H3.1 becomes associated with viral DNA
451 accompanied with viral DNA replication (28). It is suggested that this functional link
452 between DNA replication and the histone deposition enables to transfer "epigenetic
453 memory" such as histone modifications to the daughter DNA strands (43). Thus, some
454 DNA viruses might take advantage of this system for late gene expression, which
455 generally occurs after viral DNA replication. On the other hand, Ad seems to utilize
456 another strategy, that is, the uncoupling mechanism, as shown here. Like other DNA
457 viruses, Ad late genes are expressed only after the onset of viral DNA replication.
458 Thomas and Mathews demonstrated that Ad late gene expression requires its DNA
459 replication in *cis* (45), although the molecular mechanism remains to be determined.
460 This report leads us to hypothesize that the regulation of viral chromatin structure
461 during DNA replication could be an important process for the late gene expression. In
462 general, histone/nucleosome structure on DNA restricts the access of *trans*-acting
463 factors, such as transciption factors. In this view, DBP is an attractive candidate of the
464 key regulatory factor for DNA replication-dependent expression of viral late genes.
465 By oligomerization, DBP is able to not only support viral DNA replication, but also
466 establish the "histone-free" environment, which could be an opportunity window for

467 transcription factors to access the viral DNA for the activation of viral late genes. Our
468 IF analyses showed that transcription factor USF1, which binds to the MLP region after
469 viral DNA replication (46), are not excluded from VDRF (Fig. 5B and C), supporting
470 this notion. Further, this is in agreement with the report that DBP enhances the
471 binding of USF1 to the MLP region *in vitro* (51). Overall, we speculate that
472 uncoupling of the histone deposition with viral DNA replication is mediated by DBP
473 oligomerization, at least partly, and plays a role in DNA replication-dependent
474 activation of viral late gene expression.

475 The expression of certain cellular genes, such as *HoxB* gene, is shown to
476 require DNA replication (12). However, the regulation mechanism of "DNA
477 replication-dependent gene expression" remains to be determined. As Ad has late
478 genes, the expression of which are DNA replication-dependent (45), this virus could be
479 a good model for the analyses of such regulations. Therefore, this study might give a
480 clue for understanding the functional relationship between DNA replication and
481 transcription on cellular and/or viral chromatin.
482

ACKNOWLEDGMENTS

We thank Drs. M. Okuwaki, S. Saito, A. Verreault, and W. C. Russel, and K. Kajitani for their kind gifts. This work was supported in part by Grants-in-aid for Scientific Research from the Ministry of Education, Culture, Sports, Science and Technology of Japan (to K.N.) and the University of Tsukuba Research Infrastructure Support Program (to T.K.).

REFERECES

1. **Ahmad, K., and S. Henikoff.** 2002. The histone variant H3.3 marks active chromatin by replication-independent nucleosome assembly. Mol Cell **9:**1191-200.
2. **Bell, O., V. K. Tiwari, N. H. Thoma, and D. Schubeler.** 2011. Determinants and dynamics of genome accessibility. Nat Rev Genet **12:**554-64.
3. **Beyer, A. L., A. H. Bouton, L. D. Hodge, and O. L. Miller, Jr.** 1981. Visualization of the major late R strand transcription unit of adenovirus serotype 2. J Mol Biol **147:**269-95.
4. **Burg, J. L., J. Schweitzer, and E. Daniell.** 1983. Introduction of superhelical turns into DNA by adenoviral core proteins and chromatin assembly factors. J Virol **46:**749-55.
5. **Carson, C. T., N. I. Orazio, D. V. Lee, J. Suh, S. Bekker-Jensen, F. D. Araujo, S. S. Lakdawala, C. E. Lilley, J. Bartek, J. Lukas, and M. D. Weitzman.** 2009. Mislocalization of the MRN complex prevents ATR signaling during adenovirus infection. EMBO J **28:**652-62.
6. **Carvalho, T., J. S. Seeler, K. Ohman, P. Jordan, U. Pettersson, G. Akusjarvi, M. Carmo-Fonseca, and A. Dejean.** 1995. Targeting of adenovirus E1A and E4-ORF3 proteins to nuclear matrix-associated PML bodies. J Cell Biol **131:**45-56.
7. **Chatterjee, P. K., M. E. Vayda, and S. J. Flint.** 1986. Adenoviral protein VII packages intracellular viral DNA throughout the early phase of infection. EMBO J **5:**1633-44.
8. **Cherubini, G., V. Naim, P. Caruso, R. Burla, M. Bogliolo, E. Cundari, K. Benihoud, I. Saggio, and F. Rosselli.** 2011. The FANC pathway is activated by adenovirus infection and promotes viral replication-dependent recombination. Nucleic Acids Res **39:**5459-73.
9. **Dekker, J., P. N. Kanellopoulos, A. K. Loonstra, J. A. van Oosterhout, K. Leonard, P. A. Tucker, and P. C. van der Vliet.** 1997. Multimerization of the adenovirus DNA-binding protein is the driving force for ATP-independent DNA unwinding during strand displacement synthesis. EMBO J **16:**1455-63.
10. **Drane, P., K. Ouararhni, A. Depaux, M. Shuaib, and A. Hamiche.** 2010. The

death-associated protein DAXX is a novel histone chaperone involved in the replication-independent deposition of H3.3. Genes Dev **24:**1253-65.

11. **Elsaesser, S. J., A. D. Goldberg, and C. D. Allis.** 2010. New functions for an old variant: no substitute for histone H3.3. Curr Opin Genet Dev **20:**110-7.

12. **Fisher, D., and M. Mechali.** 2003. Vertebrate HoxB gene expression requires DNA replication. EMBO J **22:**3737-48.

13. **Giberson, A. N., A. R. Davidson, and R. J. Parks.** 2011. Chromatin structure of adenovirus DNA throughout infection. Nucleic Acids Res (in press). doi: 10.1093/nar/gkr1076.

14. **Groth, A., W. Rocha, A. Verreault, and G. Almouzni.** 2007. Chromatin challenges during DNA replication and repair. Cell **128:**721-33.

15. **Gyurcsik, B., H. Haruki, T. Takahashi, H. Mihara, and K. Nagata.** 2006. Binding modes of the precursor of adenovirus major core protein VII to DNA and template activating factor I: implication for the mechanism of remodeling of the adenovirus chromatin. Biochemistry **45:**303-13.

16. **Hake, S. B., and C. D. Allis.** 2006. Histone H3 variants and their potential role in indexing mammalian genomes: the "H3 barcode hypothesis". Proc Natl Acad Sci U S A **103:**6428-35.

17. **Haruki, H., B. Gyurcsik, M. Okuwaki, and K. Nagata.** 2003. Ternary complex formation between DNA-adenovirus core protein VII and TAF-Ibeta/SET, an acidic molecular chaperone. FEBS Lett **555:**521-7.

18. **Haruki, H., M. Okuwaki, M. Miyagishi, K. Taira, and K. Nagata.** 2006. Involvement of template-activating factor I/SET in transcription of adenovirus early genes as a positive-acting factor. J Virol **80:**794-801.

19. **Kawase, H., M. Okuwaki, M. Miyaji, R. Ohba, H. Handa, Y. Ishimi, T. Fujii-Nakata, A. Kikuchi, and K. Nagata.** 1996. NAP-I is a functional homologue of TAF-I that is required for replication and transcription of the adenovirus genome in a chromatin-like structure. Genes Cells **1:**1045-56.

20. **Komatsu, T., H. Haruki, and K. Nagata.** 2011. Cellular and viral chromatin proteins are positive factors in the regulation of adenovirus gene expression. Nucleic Acids Res **39:**889-901.

21. **Lewis, P. W., S. J. Elsaesser, K. M. Noh, S. C. Stadler, and C. D. Allis.** 2010. Daxx is an H3.3-specific histone chaperone and cooperates with ATRX in

replication-independent chromatin assembly at telomeres. Proc Natl Acad Sci U S A **107:**14075-80.

22. **Matsumoto, K., K. Nagata, M. Ui, and F. Hanaoka.** 1993. Template activating factor I, a novel host factor required to stimulate the adenovirus core DNA replication. J Biol Chem **268:**10582-7.

23. **Matsumoto, K., M. Okuwaki, H. Kawase, H. Handa, F. Hanaoka, and K. Nagata.** 1995. Stimulation of DNA transcription by the replication factor from the adenovirus genome in a chromatin-like structure. J Biol Chem **270:**9645-50.

24. **Nagata, K., H. Kawase, H. Handa, K. Yano, M. Yamasaki, Y. Ishimi, A. Okuda, A. Kikuchi, and K. Matsumoto.** 1995. Replication factor encoded by a putative oncogene, set, associated with myeloid leukemogenesis. Proc Natl Acad Sci U S A **92:**4279-83.

25. **Nitzsche, A., C. Paulus, and M. Nevels.** 2008. Temporal dynamics of cytomegalovirus chromatin assembly in productively infected human cells. J Virol **82:**11167-80.

26. **Okuwaki, M., A. Iwamatsu, M. Tsujimoto, and K. Nagata.** 2001. Identification of nucleophosmin/B23, an acidic nucleolar protein, as a stimulatory factor for in vitro replication of adenovirus DNA complexed with viral basic core proteins. J Mol Biol **311:**41-55.

27. **Okuwaki, M., and K. Nagata.** 1998. Template activating factor-I remodels the chromatin structure and stimulates transcription from the chromatin template. J Biol Chem **273:**34511-8.

28. **Placek, B. J., J. Huang, J. R. Kent, J. Dorsey, L. Rice, N. W. Fraser, and S. L. Berger.** 2009. The histone variant H3.3 regulates gene expression during lytic infection with herpes simplex virus type 1. J Virol **83:**1416-21.

29. **Polo, S. E., D. Roche, and G. Almouzni.** 2006. New histone incorporation marks sites of UV repair in human cells. Cell **127:**481-93.

30. **Polo, S. E., S. E. Theocharis, J. Klijanienko, A. Savignoni, B. Asselain, P. Vielh, and G. Almouzni.** 2004. Chromatin assembly factor-1, a marker of clinical value to distinguish quiescent from proliferating cells. Cancer Res **64:**2371-81.

31. **Pombo, A., J. Ferreira, E. Bridge, and M. Carmo-Fonseca.** 1994. Adenovirus replication and transcription sites are spatially separated in the nucleus of

588 infected cells. EMBO J **13:**5075-85.
589 32. **Ray-Gallet, D., J. P. Quivy, C. Scamps, E. M. Martini, M. Lipinski, and G.**
590 **Almouzni.** 2002. HIRA is critical for a nucleosome assembly pathway
591 independent of DNA synthesis. Mol Cell **9:**1091-100.
592 33. **Ray-Gallet, D., A. Woolfe, I. Vassias, C. Pellentz, N. Lacoste, A. Puri, D. C.**
593 **Schultz, N. A. Pchelintsev, P. D. Adams, L. E. Jansen, and G. Almouzni.** 2011.
594 Dynamics of histone h3 deposition in vivo reveal a nucleosome gap-filling
595 mechanism for h3.3 to maintain chromatin integrity. Mol Cell **44:**928-41.
596 34. **Ross, P. J., M. A. Kennedy, C. Christou, M. Risco Quiroz, K. L. Poulin, and**
597 **R. J. Parks.** 2011. Assembly of helper-dependent adenovirus DNA into
598 chromatin promotes efficient gene expression. J Virol **85:**3950-8.
599 35. **Samad, M. A., T. Komatsu, M. Okuwaki, and K. Nagata.** 2012.
600 B23/Nucleophosmin is involved in regulation of adenovirus chromatin structure
601 at late infection stages, but not in its replication and transcription. J Gen Virol
602 (in press). doi: 10.1099/vir.0.036665-0.
603 36. **Samad, M. A., M. Okuwaki, H. Haruki, and K. Nagata.** 2007. Physical and
604 functional interaction between a nucleolar protein nucleophosmin/B23 and
605 adenovirus basic core proteins. FEBS Lett **581:**3283-8.
606 37. **Sawatsubashi, S., T. Murata, J. Lim, R. Fujiki, S. Ito, E. Suzuki, M. Tanabe,**
607 **Y. Zhao, S. Kimura, S. Fujiyama, T. Ueda, D. Umetsu, T. Ito, K. Takeyama,**
608 **and S. Kato.** 2010. A histone chaperone, DEK, transcriptionally coactivates a
609 nuclear receptor. Genes Dev **24:**159-70.
610 38. **Schreiner, S., R. Martinez, P. Groitl, F. Rayne, R. Vaillant, P. Wimmer, G.**
611 **Bossis, T. Sternsdorf, L. Marcinowski, Z. Ruzsics, T. Dobner, and H.**
612 **Wodrich.** 2012. Transcriptional Activation of the Adenoviral Genome Is
613 Mediated by Capsid Protein VI. PLoS Pathog **8:**e1002549.
614 39. **Schreiner, S., P. Wimmer, H. Sirma, R. D. Everett, P. Blanchette, P. Groitl,**
615 **and T. Dobner.** 2010. Proteasome-dependent degradation of Daxx by the viral
616 E1B-55K protein in human adenovirus-infected cells. J Virol **84:**7029-38.
617 40. **Shibahara, K., and B. Stillman.** 1999. Replication-dependent marking of DNA
618 by PCNA facilitates CAF-1-coupled inheritance of chromatin. Cell **96:**575-85.
619 41. **Smith, S., and B. Stillman.** 1989. Purification and characterization of CAF-I, a
620 human cell factor required for chromatin assembly during DNA replication in

vitro. Cell **58:**15-25.

42. **Stracker, T. H., D. V. Lee, C. T. Carson, F. D. Araujo, D. A. Ornelles, and M. D. Weitzman.** 2005. Serotype-specific reorganization of the Mre11 complex by adenoviral E4orf3 proteins. J Virol **79:**6664-73.

43. **Tagami, H., D. Ray-Gallet, G. Almouzni, and Y. Nakatani.** 2004. Histone H3.1 and H3.3 complexes mediate nucleosome assembly pathways dependent or independent of DNA synthesis. Cell **116:**51-61.

44. **Takami, Y., T. Ono, T. Fukagawa, K. Shibahara, and T. Nakayama.** 2007. Essential role of chromatin assembly factor-1-mediated rapid nucleosome assembly for DNA replication and cell division in vertebrate cells. Mol Biol Cell **18:**129-41.

45. **Thomas, G. P., and M. B. Mathews.** 1980. DNA replication and the early to late transition in adenovirus infection. Cell **22:**523-33.

46. **Toth, M., W. Doerfler, and T. Shenk.** 1992. Adenovirus DNA replication facilitates binding of the MLTF/USF transcription factor to the viral major late promoter within infected cells. Nucleic Acids Res **20:**5143-8.

47. **Tucker, P. A., D. Tsernoglou, A. D. Tucker, F. E. Coenjaerts, H. Leenders, and P. C. van der Vliet.** 1994. Crystal structure of the adenovirus DNA binding protein reveals a hook-on model for cooperative DNA binding. EMBO J **13:**2994-3002.

48. **Ullman, A. J., and P. Hearing.** 2008. Cellular proteins PML and Daxx mediate an innate antiviral defense antagonized by the adenovirus E4 ORF3 protein. J Virol **82:**7325-35.

49. **Vayda, M. E., A. E. Rogers, and S. J. Flint.** 1983. The structure of nucleoprotein cores released from adenovirions. Nucleic Acids Res **11:**441-60.

50. **Verreault, A., P. D. Kaufman, R. Kobayashi, and B. Stillman.** 1996. Nucleosome assembly by a complex of CAF-1 and acetylated histones H3/H4. Cell **87:**95-104.

51. **Zijderveld, D. C., F. d'Adda di Fagagna, M. Giacca, H. T. Timmers, and P. C. van der Vliet.** 1994. Stimulation of the adenovirus major late promoter in vitro by transcription factor USF is enhanced by the adenovirus DNA binding protein. J Virol **68:**8288-95.

654

655

656 **FIGURE LEGENDS**

657 **FIG. 1. Viral chromatin structure in early and late phases of infection.** (A)
658 The structure of Ad genome. Arrows represent promoters of viral genes. Target
659 regions for ChIP assays are indicated by arrowheads. (B) The amounts of viral DNA.
660 HeLa cells were infected with HAdV5 at an MOI of 100, and DNA samples were
661 purified from infected cells at 6 and 12 hpi. The amount of viral DNA was
662 quantitatively measured by qPCR using primers for the E1A promoter region. The
663 amount of viral DNA was graphed as the ratio relative to that at 6 hpi. (C) ChIP
664 assays. HeLa cells were infected with HAdV5 at an MOI of 100 and subjected to
665 ChIP assays using infected cells at 6 and 12 hpi. Immunoprecipitation was carried out
666 using indicated antibodies and anti-FLAG antibody (as a negative control). The
667 obtained DNAs were quantitatively measured by qPCR using indicated primer sets.
668 The binding levels of each protein were calculated as relative enrichment against that
669 obtained in a negative control (anti-FLAG antibody). (D) The binding levels of core
670 histones. Base on the results of ChIP assays shown in (C), the binding level of histone
671 H4 and H2A-H2B was normalized by that of histone H3.

672

673 **FIG. 2. Localization and role of PCNA and CAF-1 during viral DNA replication.**
674 (A) IF assays. HeLa cells and cells stably expressing HA-PCNA grown on cover
675 slips were mock-infected or infected with HAdV5 at an MOI of 50. At 18 hpi the
676 localization patterns of HA-PCNA and DBP were analyzed by IF using anti-HA and
677 anti-DBP antibodies. DNA was visualized by TO-PRO-3 iodide staining. Merged

images are also indicated. Higher-magnified images of the regions marked by squares are shown below. (B) RT-qPCR assays. HeLa cells were treated with siControl or siCAF-1 and then either mock-infected or infected with HAdV5 at an MOI of 100, and total RNAs were purified at 6 and 12 hpi. cDNAs were synthesized with reverse transcription and subjected to qPCR using primer sets for *CAF-1 p150* and *GAPDH* mRNAs. The mRNA levels relative to those in control cells at 12 hpi were graphed. (C) ChIP assays. siRNA-treated cells were infected with HAdV5 at an MOI of 100 and at 6 and 12 hpi subjected to ChIP assays using anti-histone H3 and anti-FLAG antibodies as described above. (D) Relative amounts of viral DNA. Viral DNA was purified from lysates for ChIP assays in (C) and subjected to qPCR using primer set for the E1A promoter. The DNA amounts at 12 hpi relative to those at 6 hpi were shown.

FIG. 3. Incorporation of histone H3 variants into viral chromatin. (A, B) ChIP assays with FLAG-tagged histone H3 variants. HeLa cells were transfected with pcDNA3 empty vector, pcDNA3-H3.2-FLAG, or pcDNA3-H3.3-FLAG, and at 24 hpt (hours post transfection) infected with HAdV5 at an MOI of 100. At 2, 6, and 10 hpi (A) or 12 hpi (B), ChIP assays were carried out using anti-FLAG and anti-HA (as a negative control) antibodies, as described above. Note that in the case of 10 hpi, HU was added to block viral DNA replication. The results were graphed as relative enrichment as described above. (C) Western blot analyses. At 24 hpt, lysates were prepared from cells transfected with pcDNA3 empty (lane 1), pcDNA3-H3.2-FLAG

700 (lane 2), and pcDNA3-H3.3-FLAG (lane 3) and subjected to 15% SDS-PAGE, followed
701 by western blot analyses using anti-FLAG (upper panel) and anti-β-actin (lower panel)
702 antibodies. (D) Western blot analyses. HeLa cells were transfected with pcDNA3
703 empty vector (lane 1), pcDNA3-H3.1-FLAG (Lane 2), or pcDNA3-H3.3-FLAG (lane 3),
704 and at 24 hpt lysates were prepared and subjected to 15% SDS-PAGE, followed by
705 western blot analyses using anti-FLAG (upper panel) and anti-β-actin (lower panel)
706 antibodies. (E) ChIP assays. HeLa cells transfected with pcDNA3 empty vector
707 (lanes 2, 3, 9, and 10), pcDNA3-H3.1-FLAG (lanes 4, 5, 11, and 12), or
708 pcDNA3-H3.3-FLAG (lanes 6, 7, 13, and 14) were infected with HAdV5 at an MOI of
709 100. At 10 hpi (left panels, lanes 1-7) or 12 hpi (right panels, lanes 8-14), ChIP assays
710 were carried out using anti-FLAG (lanes 3, 5, 7, 10, 12, and 14) and anti-HA (as a
711 negative control, lanes 2, 4, 6, 9, 11, and 13) antibodies. In the case of 10 hpi, HU was
712 added to block viral DNA replication. The immunoprecipitated DNAs were amplified
713 by semi-quantitative PCR using the indicated primer sets. PCR products were
714 separated on a 7% polyacrylamide gel and visualized by staining with EtBr. Input
715 DNAs (lanes 1 and 8) were purified from 0.5% of lysates of cells transfected with the
716 empty vector.
717
718 **FIG. 4. Localization of histones in late phases of infection.** (A) IF analyses
719 using cells stably expressing histone H3.3-EGFP. HeLa cells stably expressing histone
720 H3.3-EGFP grown on cover slips were mock-infected or infected at an MOI of 50, and
721 at 18 hpi subjected to IF assays using anti-DBP (upper panels) and anti-CAF-1 p150

(lower panels) antibodies, as described above. Higher-magnified images of the regions marked by squares are shown below. (B) Localization of histone H3.2 in late phases of infection. HeLa cells stably expressing histone H3.2-EGFP were mock-infected or infected with HAdV5 at an MOI of 50, and at 18 hpi subjected to IF analyses using anti-DBP antibody. Higher-magnified images of the regions marked by squares are shown. (C) Localization of endogenous histone H2A in late phases of infection. HeLa cells were mock-infected or infected with HAdV5 at an MOI of 50, and at 18 hpi subjected to IF assays using anti-histone H2A and anti-DBP antibodies. Higher-magnified images of the regions marked by squares are shown below. (D) Histone localization in early phases of infection. HeLa cells stably expressing histone H3.2-EGFP and H3.3-EGFP were mock-infected or infected with HAdV5 at an MOI of 250, and at 4 hpi subjected to IF analyses using anti-protein VII antibody.

FIG. 5. Localization of nuclear proteins in late phases of infection. (A) IF analyses using anti-HIRA antibody. HeLa cells were mock-infected or infected with HAdV5 at an MOI of 250 (for 4 hpi) or 50 (for 18 hpi) and subjected to IF analyses using anti-protein VII and anti-HIRA antibodies. (B) Western blot analyses. Lysates were prepared from HeLa cells transfected with pCHA-puro empty vector (lane 1), pCHA-DEK (Lane 2), or pCHA-puro-USF1 (lane 3) at 24 hpt, and subjected to 10% SDS-PAGE, followed by western blot analyses using anti-HA (upper panel) and anti-β-actin (lower panel) antibodies. (C) Localization of HA-DEK and HA-USF1. HeLa cells were transfected pCHA-puro empty vector, pCHA-DEK, or

744 pCHA-puro-USF1. At 24 hpt, cells were mock-infected or infected with HAdV5 at an
745 MOI of 50, and at 18 hpi subjected to IF assays using anti-HA and anti-DBP antibodies.
746
747 **FIG. 6. Role of DBP oligomerization on histone localization.** (A) Schematic
748 diagrams of full-length DBP and C-terminally deleted mutant DBPΔC. DBP of
749 HAdV5 consists of 529 aa, and the C-terminal 17 aa (513-529) functions as an "arm"
750 for oligomerization. DBPΔC lacks the C-terminal 17 aa. (B) Western blot analyses.
751 HeLa cells stably expressing histone H3.3-EGFP were transfected with pCHA-puro
752 empty vector (lane 1), pCHA-puro-DBP (lane 2), or pCHA-puro-DBPΔC (lane 3), and
753 lysates prepared at 36 hpt were subjected to 10% SDS-PAGE, followed by western blot
754 analyses using anti-HA (top), anti-DBP (middle), and anti-β-actin (bottom panel)
755 antibodies. (C) IF analyses. At 36 hpt, cells as described in (B) grown on cover
756 slips were subjected to IF analyses using anti-HA (left panels) and anti-DBP (right
757 panels) antibodies as described above. Higher-magnified images of the regions
758 marked by squares are shown below.
759
760 **FIG. 7. A hypothetical model for viral chromatin structure during infection cycle.**
761 For detail, see Discussion section.
762

Figure 1 Komatsu *et al.*

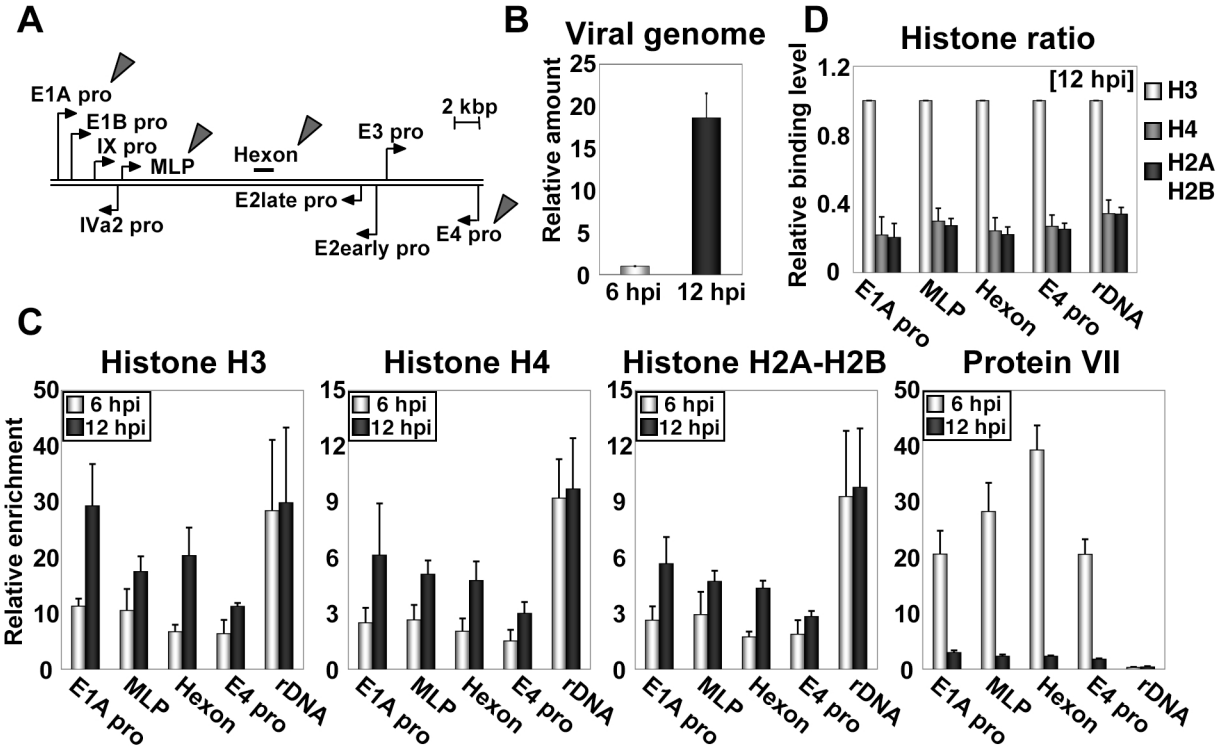

Figure 2 Komatsu *et al.*

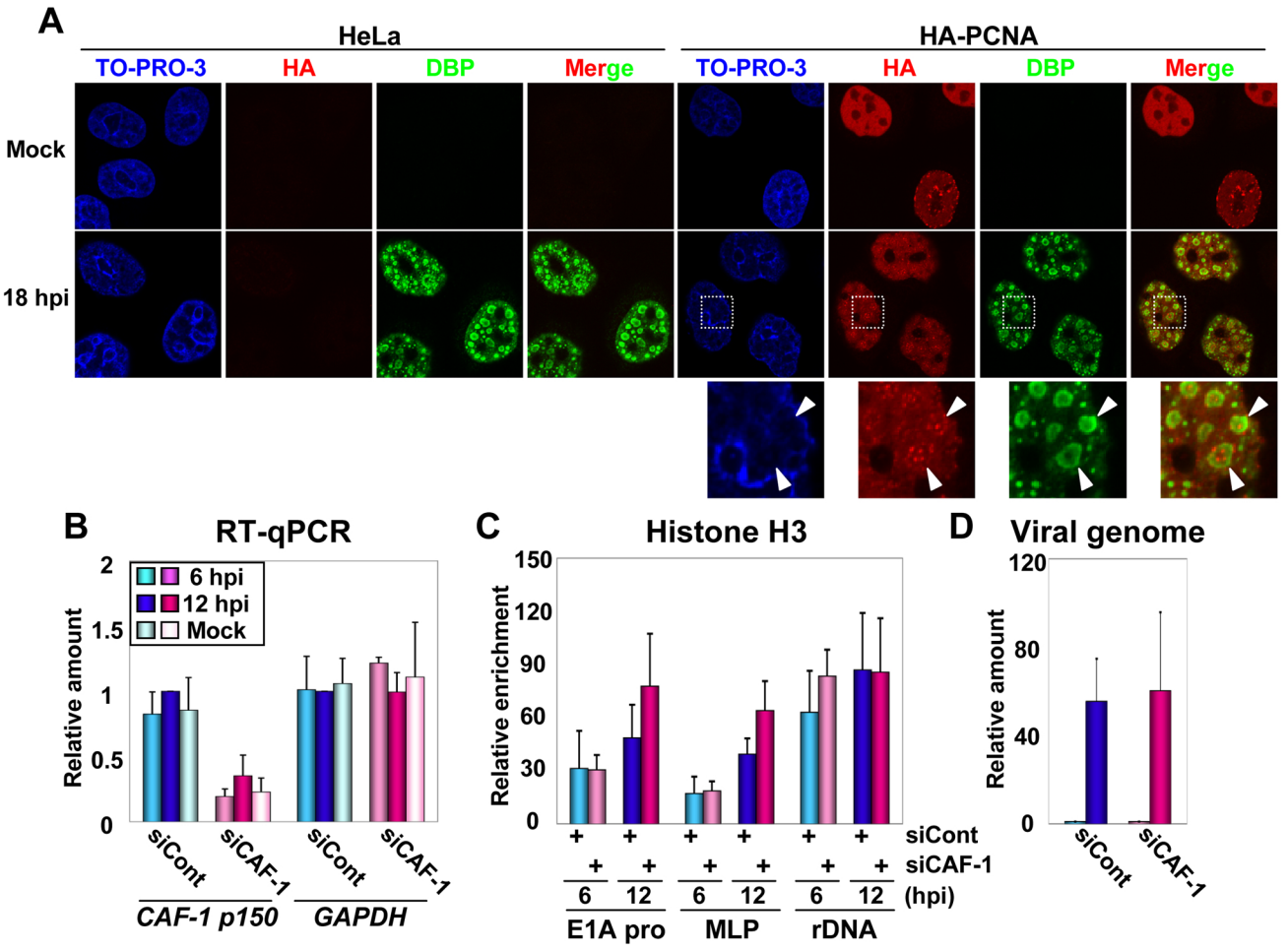

Figure 3 Komatsu *et al*.

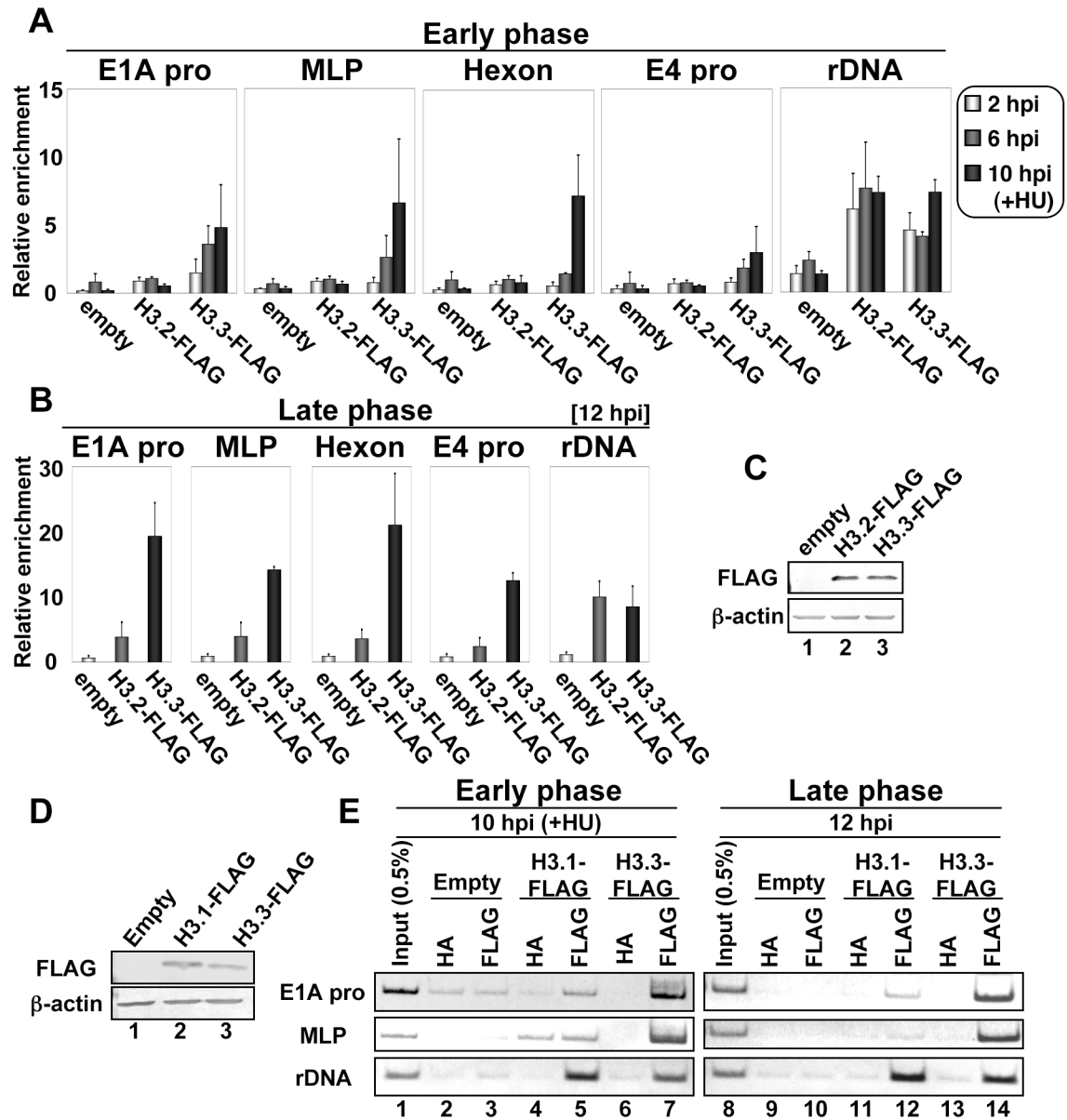

Figure 4 Komatsu *et al*.

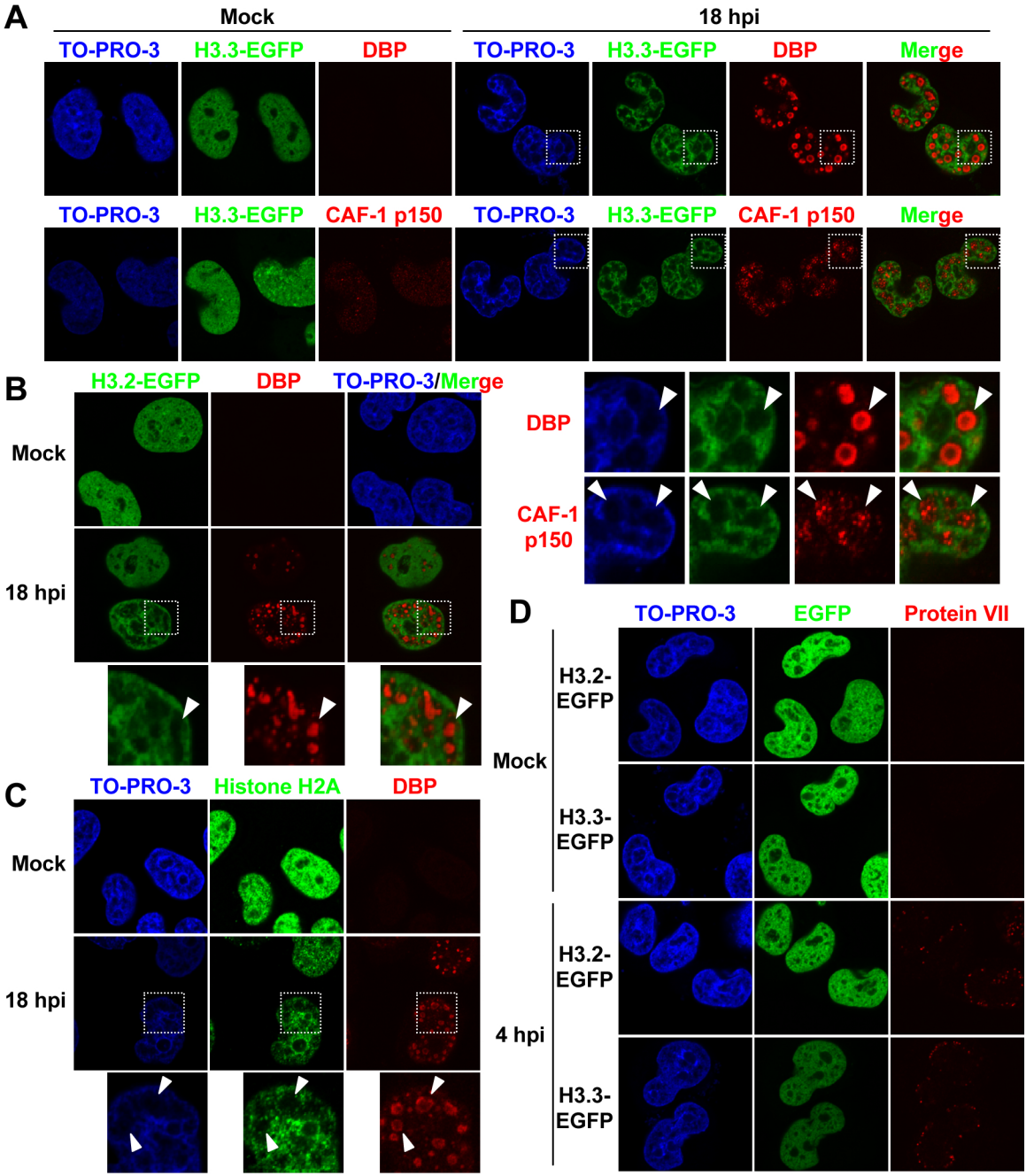

Figure 5 Komatsu *et al*.

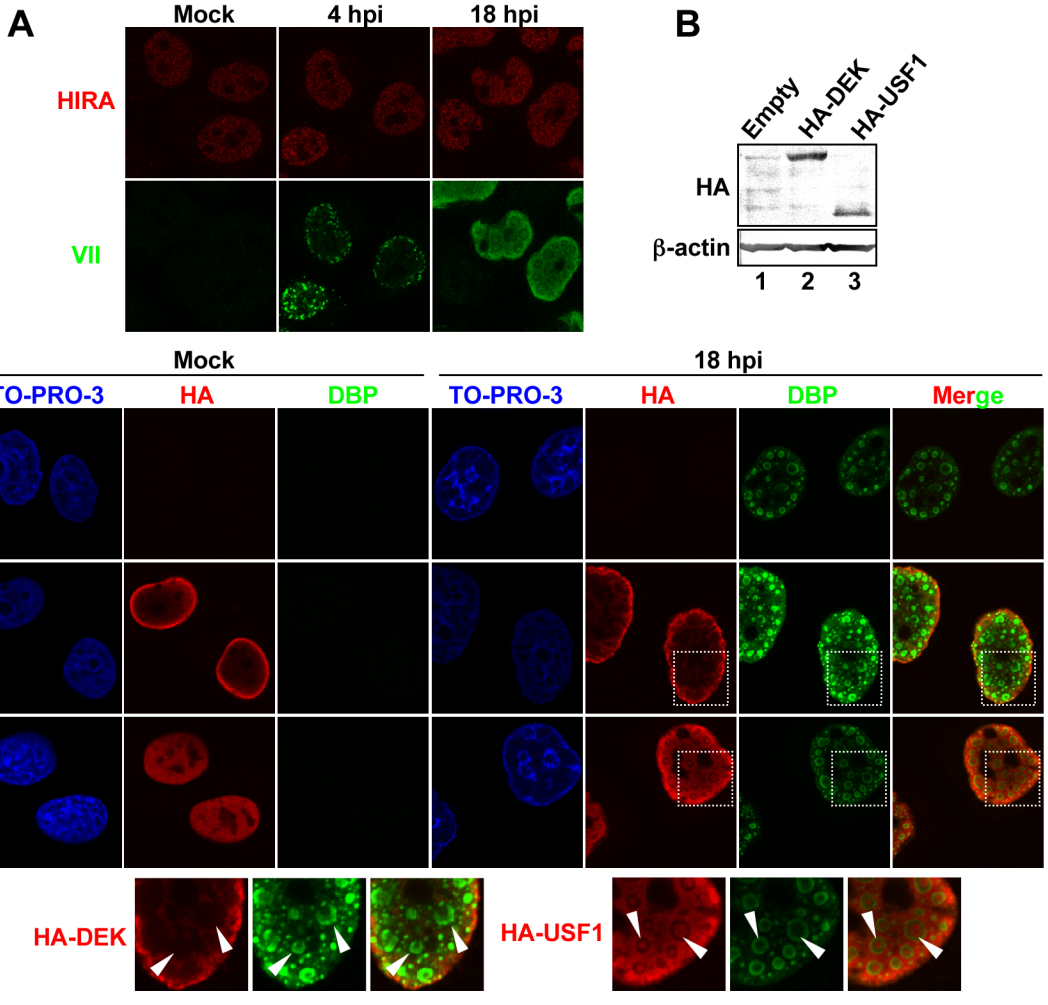

Figure 6 Komatsu *et al*.

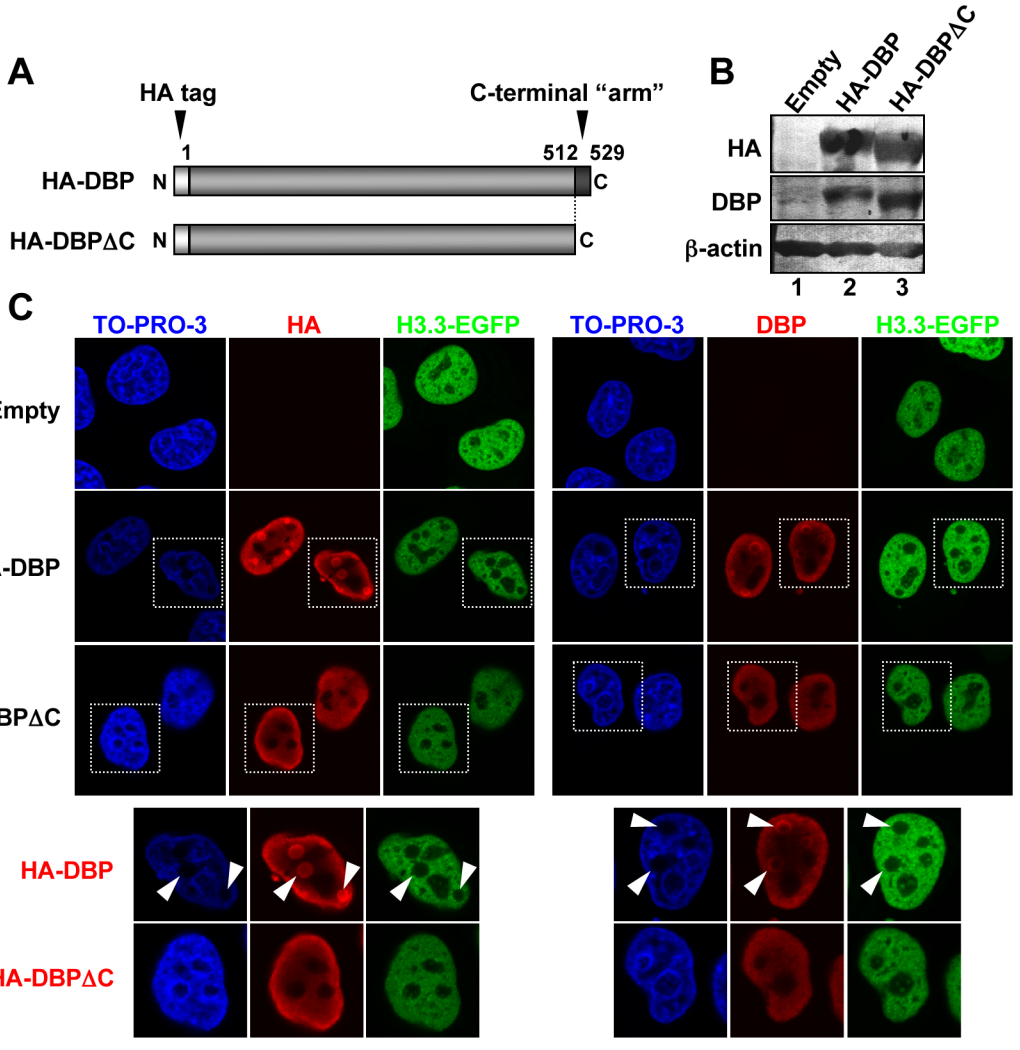

Figure 7 Komatsu *et al*.